A COMPARISON BETWEEN SPECTROSCOPIC PERFORMANCE OF HgI_2 AND CdZnTe FRISCH COLLAR DETECTORS

MATERIALS FOR NUCLEAR SYSTEMS

KEYWORDS: *CdZnTe spectrometer, HgI_2 detector, Frisch collar device*

A. KARGAR,[a]* E. ARIESANTI,[b] and D. S. McGREGOR[b]

[a]*Radiation Monitoring Devices, Inc., 44 Hunt Street, Watertown, Massachusetts 02472*
[b]*Kansas State University, Mechanical and Nuclear Engineering Department S.M.A.R.T. Laboratory, Manhattan, Kansas 66506*

Received April 18, 2010
Accepted for Publication February 8, 2011

In this study, the charge collection efficiencies (CCEs) of a 7.8- × 7.8- × 15.6-mm³ CdZnTe Frisch collar detector and a 2.1- × 2.1- × 4.1-mm³ HgI_2 Frisch collar detector were measured and compared. Two Frisch collar devices were designed and fabricated to have identical aspect ratios of 2.0 to maintain similar weighting potential distributions. Pulse-height spectra were acquired from both Frisch collar devices with a standard calibration gamma-ray source of ^{137}Cs, and the results are presented. As known, the Frisch collar alters the weighting potential within the planar device and enhances the CCE distributions. Thus, the parameters affecting these distributions have great impact on the pulse-height spectrum. The device length and mobility-lifetime product $\mu\tau$ have great impacts on CCE. Primarily, crystal (device) length L directly affects CCE because more charge carriers are trapped in longer devices with longer traveling distances. Alternatively, the better mobility-lifetime product of the charge carriers enhances CCE of the fabricated device. It is shown in this study that as a result of similarity in shape for both devices (equal aspect ratio), the weighting potential distributions resemble each other. However, as a result of the trapping effect (due to both length and $\mu\tau$), the CCE profiles are not the same, and the CdZnTe detector shows more uniform response to gamma rays and, therefore, better spectroscopic performance (even with a longer device length), which is confirmed through CCE simulations. Finally, by applying the CCE model to the HgI_2 Frisch collar device, the mobility-lifetime products $\mu_{e,h}\tau_{e,h}$ of electrons and holes were estimated to be 0.0008 and 0.00003 $cm^2 \cdot V^{-1}$, respectively, for the HgI_2 crystal.

I. INTRODUCTION

In this study, the spectroscopic performance of a 7.8- × 7.8- × 15.6-mm³ CdZnTe Frisch collar detector is compared with a 2.1- × 2.1- × 4.1-mm³ HgI_2 Frisch collar detector. It was shown previously that CdZnTe and HgI_2 planar devices can be turned into single carrier devices by applying Frisch collars to the planar detectors.[1,2] The Frisch collar alters the weighting potential within the device and enhances the charge collection efficiency (CCE) distributions. This enhancement in spectroscopic performance is mainly due to a uniformity of the response to the gamma rays over the Frisch collar device length.[3]

Because the device aspect ratio *AR* (length-to-width ratio) is one of the most important parameters in determining the weighting potential distribution, and consequently CCE, the ideal *AR*s of both devices were determined to be 2, as described elsewhere.[4,5] It has been shown previously that for the CdZnTe Frisch collar devices with the same aspect ratio and similar electron transport properties, the shorter devices show more uniform responses to gamma rays.[4] Despite equal *AR*s for both devices in this study and a shorter length for the HgI_2 Frisch collar detector, the CdZnTe Frisch collar device shows better spectroscopic performance compared to its HgI_2

*E-mail: AKargar@RMDInc.com

counterpart. This advantage is mainly due to a better electron mobility-lifetime product $\mu\tau$. Nevertheless, both CdZnTe and HgI_2 Frisch collar detectors showed excellent spectroscopic performance when compared to their operation as planar devices.

For some specific applications where a large detecting area is desired, pixelated devices are the most commonly used method.[6,7] However, there are several issues with large detectors using pixelated devices. First, acquiring a large-volume single crystal can be costly, especially when the crystal is difficult to grow, and hence, the material is not readily available. Second, the crystal may require very expensive and complicated readout electronics. Third, fabricating and handling a large-volume pixelated device is also time-consuming and requires complicated equipment. Fourth, there are some technical issues and limitations with pixelated devices, such as charge-sharing and cross-talking.

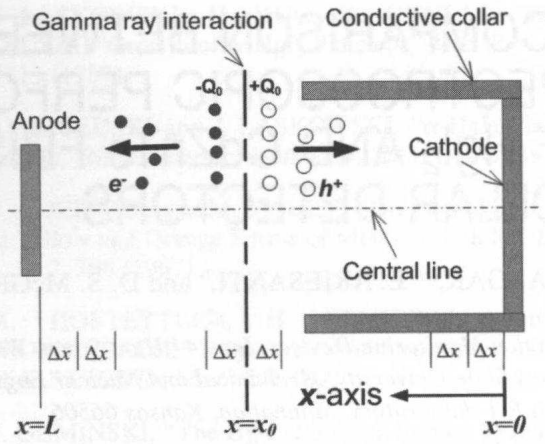

Fig. 1. Application of Shockley-Ramo theorem to a two-dimensional Frisch collar device along the central axis. The conductive Frisch collar is coupled to the cathode, and both are grounded, while the collar covers the entire lateral side of both devices.

II. THEORY

The CCE at a given point x_0, $CCE(x_0)$, within a gamma-ray detector and along the device central line is defined as the normalized change in induced charge between the interaction location x_0 and the collecting electrode. For instance, if Q_0 is generated by a single photon interaction at point x_0 within the device and $Q_t(x_0)$ is the total induced charge sensed by the collecting electrode after the remaining charges are collected, including trapping effects, then the CCE at point x_0, $CCE(x_0)$ is defined by

$$CCE(x_0) = \frac{Q_t(x_0)}{Q_0} \quad . \tag{1}$$

In most compound semiconductors, there is significant charge carrier trapping that degrades the device performance because of incomplete and nonuniform charge collection. Therefore, the CCE is typically smaller than unity.

The electron and hole contribution to charge induction is the summation of the change in induced charge due to electron motion ΔQ_e and the change in induced charge due to hole motion ΔQ_h over the *entire* path of their motion from where they are generated at x_0, until they are trapped or collected (see Fig. 1). In other words, if an interaction occurs at x_0 within the detector, then the holes travel from point x_0 to the cathode, while the electrons travel from x_0 to the anode. By applying the Shockley-Ramo theorem,[8,9] the contribution of electrons and holes to the change in induced charge can be defined as small differences over the entire length of the device L as

$$\Delta Q_{e,h}(x_{i+1}) = \Delta\psi(x_{i+1}, x_i)\, Q(x_{i+1}) \quad , \tag{2}$$

where x_{i+1} is the position of the charge carriers as they travel incrementally from x_i. In Eq. (2), $\psi(x)$ is the weighting potential distribution, which can be evaluated by using Laplace's equation,

$$\nabla\cdot[\kappa_i \epsilon_0 \nabla\psi] = 0 \quad , \tag{3}$$

with the boundary conditions of $\psi = 1$ at the collecting electrode, and $\psi = 0$ for all other electrodes, where κ_i is the dielectric constant of material i. The weighting potential distributions for the 7.8- × 7.8- × 15.6-mm^3 CdZnTe Frisch collar detector and the 2.1- × 2.1- × 4.1-mm^3 HgI_2 Frisch collar detector are plotted in Fig. 2. On the other hand, as charge carriers move, they are trapped, and the effect of trapping can be considered as the following description. If charge Q_0 exists at time $t = 0$ at x_0, the amount of charge $Q(t)$ at time $t = \Delta t$ is

$$Q(t) = Q_0 \exp\left[\frac{-\Delta t}{\tau}\right] \quad . \tag{4}$$

By considering either of these weighting potential distributions, the total induced charge $Q_t(x_0)$, due to Q_0 charges generated at x_0, is

$$Q_t(x_0) = \sum_{x_i=x_0}^{Anode} \Delta Q_e(x_i) + \sum_{x_i=x_0}^{Cathode} \Delta Q_h(x_i) \quad , \tag{5}$$

where x is the position of the charge carriers. Note that appropriate signs are needed for the charge carrier type (negative or positive) and the direction of the charge carrier. Applying Eqs. (1) through (5), while considering the effect of trapping,[3,10] allows for calculation of the CCE for any symmetric device, given the material properties,[4,11] device electrodes,[11] device geometry,[4,5] and applied voltage.[12,13]

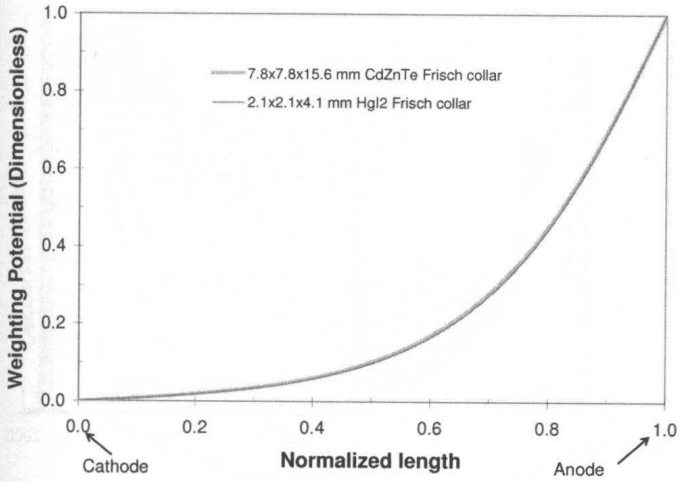

Fig. 2. The weighting potential distributions along the central axis of the CdZnTe and HgI_2 Frisch collar devices with aspect ratios of ~2 and different crystal lengths. Both distributions were calculated using LORENTZ, while considering different thicknesses of insulator layer proportional to Frisch collar device lengths. The graph shows that the weighting potential distributions for Frisch collar devices with the same aspect ratio but different lengths are identical.

A commercial simulation package from Integrated Engineering Software, LORENTZ, was employed to obtain full three-dimensional potential models of the devices in this study. A FORTRAN code was written to produce the CCE distribution, where the weighting potential distribution along the device's central line, obtained from the LORENTZ calculations, was the input. Other input parameters to model the CCE using the FORTRAN code, such as the electrical property of the semiconductor material $\mu_{e,h}\tau_{e,h}$, device length L, and the number of segments n, are entered within the FORTRAN code main body. Also noteworthy, the number of segments n (see Fig. 1) needs to be the same for both the FORTRAN code and the outputs of LORENTZ and was considered to be 1000 nodes.

III. EXPERIMENTAL PROCEDURE

III.A. Device Preparation and Setup

The HgI_2 crystals for this study were grown in the Semiconductor Materials and Radiological Technologies (S.M.A.R.T.) Laboratory at Kansas State University,[2] while the CdZnTe material was obtained from Redlen Technologies.[14] Both HgI_2 and CdZnTe Frisch collar devices were fabricated and characterized in situ in the S.M.A.R.T. Laboratory. The details of the fabrication process are reported elsewhere.[2,15]

The CCE characterization for both HgI_2 and CdZnTe Frisch collar detectors was performed using a 43.0- × 43.0- × 43.0-mm^3 Pb collimator. The collimator had a 0.6-mm-diam hole and was placed in such a way that there was an 8.7-mm gap between the detectors and the collimator. The arrangement allowed for the detectors to be irradiated with a ^{137}Cs gamma-ray source over a 0.72-mm-diam circular area (see Fig. 3). The Pb collimator was mounted on a linear stage with two degrees of freedom; hence, the Frisch collar devices could be probed by the highly collimated source at 0.65-mm increments along the device length. The Frisch collar detectors were placed 8.7 mm away from the Pb collimator and were held in place for the entire experiment, while the ^{137}Cs gamma-ray source was aligned with the collimator hole. The detector, gamma-ray source, Pb collimator, and linear stage were placed inside an aluminum test box.

III.B. Charge Collection Efficiency Measurement

The HgI_2 and CdZnTe Frisch collar devices were probed with the highly collimated ^{137}Cs gamma-ray source to investigate the response uniformity of the Frisch collar devices to high-energy gamma rays. Each Frisch collar detector and the linear stage were placed inside an aluminum test box, while the detector was connected to an eV-550 preamplifier through an SHV connector. The aluminum test box and the preamplifier were then placed inside a copper Faraday cage, and the preamplifier was connected to a high-voltage supply, amplifier, and pulse

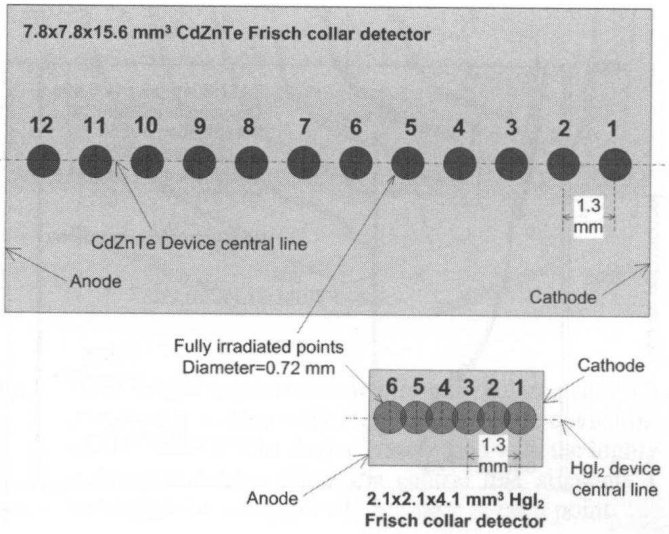

Fig. 3. The irradiated points on the 7.8- × 7.8- × 15.6-mm^3 CdZnTe Frisch collar device and the 2.1- × 2.1- × 4.1-mm^3 HgI_2 Frisch collar device for the CCE measurement. The collimated gamma-ray source on a linear stage allowed for irradiating the desired points shown on both devices. The CdZnTe and HgI_2 Frisch collar devices were irradiated in increments of 1.3 and 0.65 mm, respectively, along the device's central line.

generator. An oscilloscope, multichannel analyzer, and personal computer were used to monitor and acquire the data. Before probing the devices for the CCE experiments, a ^{137}Cs spectrum was taken with each Frisch collar device, with the gamma-ray source placed near the cathode of the device.

To conduct the CCE experiment, the lateral sides of the devices were probed with the collimated 662-keV gamma rays. Pulse-height spectra were collected for the HgI_2 detector over 4 h real time at 1500-V bias and for 2 h real time at 1700-V bias for the CdZnTe detector. It should be noted that the the HgI_2 detector was biased at 1500 V for 24 h (see Ref. 2) before collecting the pulse-height spectra. The amplifier gain was set to 69X for all measurements. The source was displaced by moving the collimated source using the two-dimensional linear stage in increments of 0.65 mm along the length of the device (points 1 through 6) for the HgI_2 detector. The same procedure was repeated for the CdZnTe detector in increments of 1.3 mm for the CdZnTe detector (points 1 through 12) as shown in Fig. 3.

IV. RESULTS AND DISCUSSION

IV.A. Pulse-Height Spectra

Figures 4 and 5 show the ^{137}Cs spectra taken with the CdZnTe and HgI_2 Frisch collar detectors, respectively, while both devices were fully irradiated (no collimation) with the gamma-ray source from the cathode side. Notice that the CdZnTe Frisch collar device has a higher energy resolution and peak-to-valley ratio, thus a better performance, compared to the HgI_2 Frisch collar device.

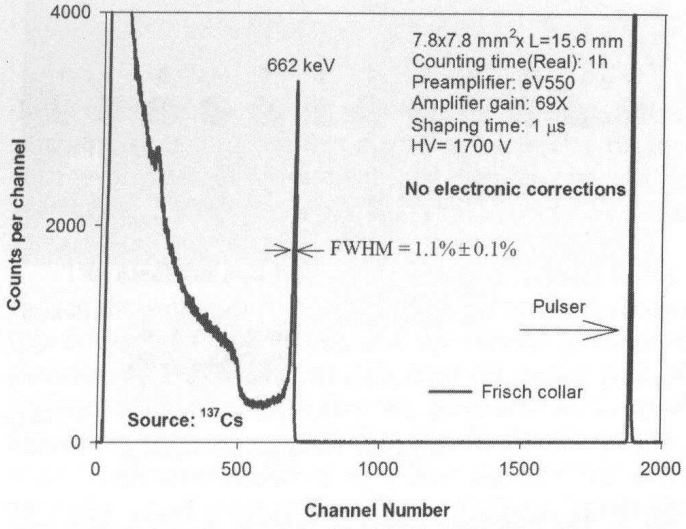

Fig. 4. A pulse-height spectrum of ^{137}Cs taken with the CdZnTe Frisch collar device ($7.8 \times 7.8 \times 15.6\ mm^3$) for 1 h real counting time. The device was fully irradiated (no collimation) with the gamma-ray source at the cathode. A 1.1% full-width at half-maximum (FWHM) energy resolution is achieved at 662 keV after the Frisch collar device was biased at 1700 V.

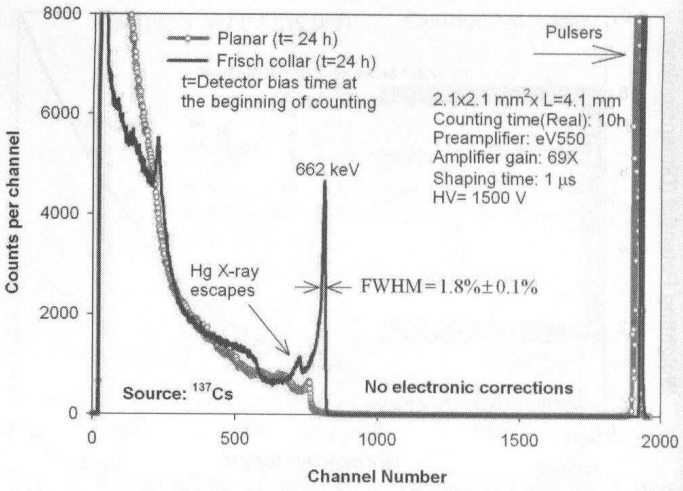

Fig. 5. The ^{137}Cs pulse-height spectra taken with the HgI_2 device ($2.1 \times 2.1 \times 4.1\ mm^3$) in both Frisch collar and planar configurations for 10 h real counting time. The device was fully irradiated (no collimation) with the gamma-ray source at the cathode. A 1.8% full-width at half-maximum (FWHM) energy resolution is achieved at 662 keV after the Frisch collar device was biased at 1500 V for 24 h (see Ref. 2). The spectra clearly show the performance enhancement due to the application of the Frisch collar to the planar device.

IV.B. Comparison of the CCE Prediction to the Photopeak Channel for the CdZnTe Frisch Collar Device

The collected spectra in Figs. 6 and 7 for the CdZnTe Frisch collar device show the uniformity of the device response to gamma rays. This uniformity is further confirmed by plotting the normalized peak channel number of each spectrum versus the irradiated points (Fig. 8). As plotted in Fig. 8 the peak channel of the photopeak remained unchanged as the collimated gamma-ray source probed more than half of the device length (points 1 through 7). The comparison between the experimentally obtained CCE and the theoretical predicted values, as shown in Fig. 8, reveals that the device response follows the prediction. For the CCE calculation, the mobility-lifetime products $\mu_{e,h}\tau_{e,h}$ of 0.045 and 0.0001 $cm^2 \cdot V^{-1}$ are used for the electrons and holes in CdZnTe, respectively; as provided by Redlen Technologies[14] and the previous studies.[3,12]

IV.C. Comparison of the CCE Prediction to the Photopeak Channel for the HgI_2 Frisch Collar Device

Figures 9 and 10 show ^{137}Cs spectra from the collimated gamma-ray source collected with the HgI_2 Frisch collar device operated at 1500 V. Similar to the results for

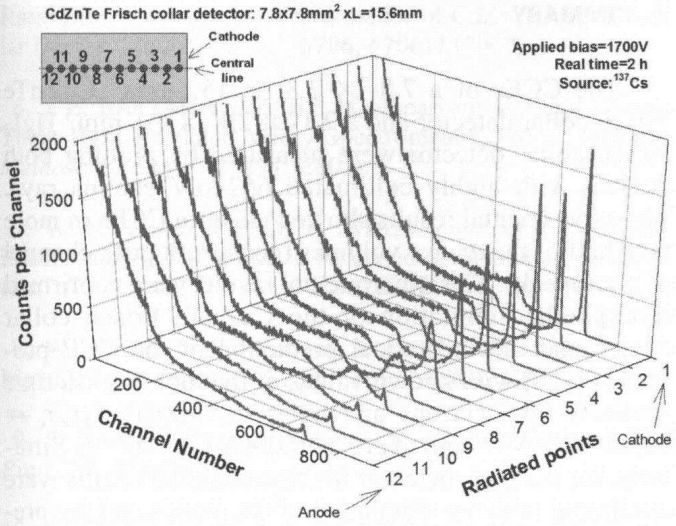

Fig. 6. Pulse-height spectra collected from the collimated ^{137}Cs gamma-ray source with the 7.8- × 7.8- × 15.6-mm^3 CdZnTe Frisch collar device biased at 1700 V. The device was probed with the highly collimated source along the central line at points 1 through 12 for 1 h real counting time at each point.

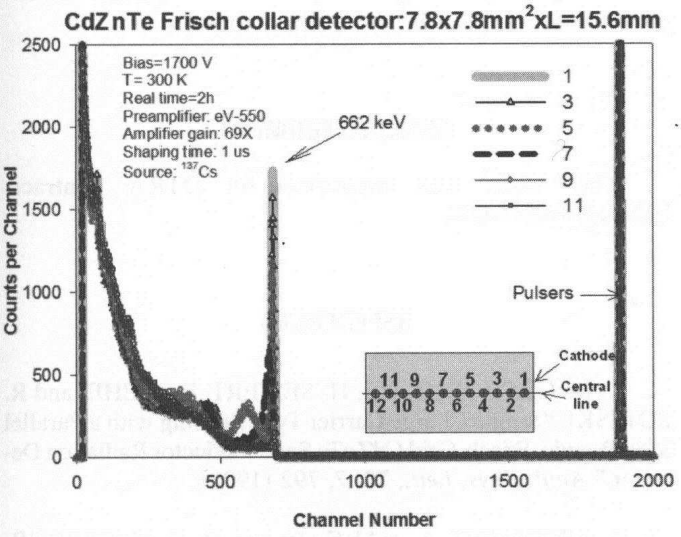

Fig. 7. Pulse-height spectra collected from the collimated ^{137}Cs gamma-ray source with the CdZnTe Frisch collar device.

the CdZnTe device, the collected spectra show the uniformity of the device response to gamma rays along the device length. This uniformity is further confirmed by plotting the normalized peak channel number of each spectrum versus the irradiated points (Fig. 11). As plotted in Fig. 11, the peak channel of the photopeak remained unchanged as the collimated gamma-ray source probed more than half of the device length (points 1 through 4). Applying the CCE model presented in Secs. II and IV.B to the 2.1- × 2.1- × 4.1-mm^3 HgI_2 Frisch collar

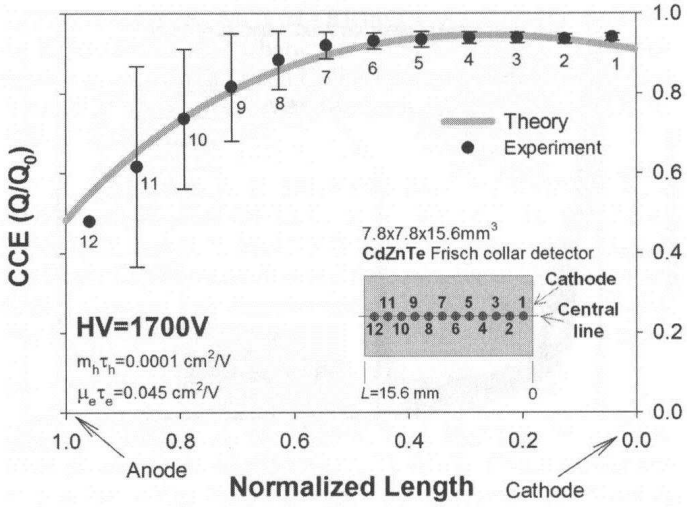

Fig. 8. The CCE profile along the central line of the CdZnTe Frisch collar device biased at 1700 V. The experimental data points are the normalized peak channel of the photopeak for the irradiated points (1 through 12) of the Frisch collar device. The error bars represent the photopeak full-width at half-maximum at 662 keV for the collected spectrum at that point. The mobility-lifetime products $\mu_{e,h}\tau_{e,h}$ of 0.045 and 0.0001 $cm^2 \cdot V^{-1}$ are assumed for the electrons and holes, respectively.

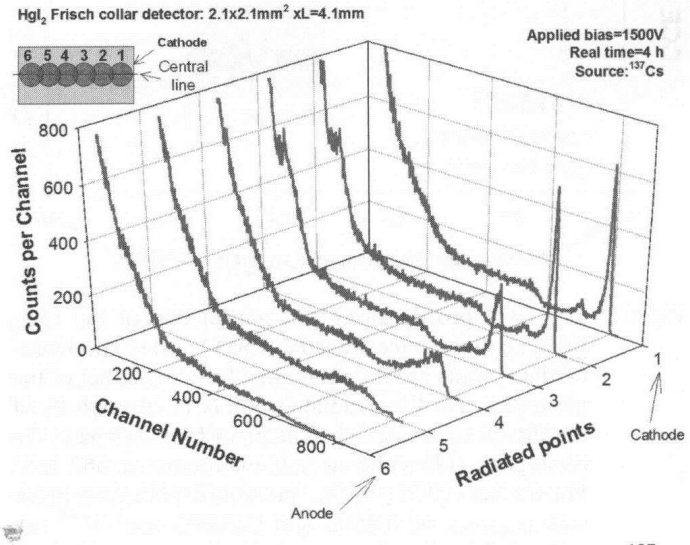

Fig. 9. Pulse-height spectra collected from the collimated ^{137}Cs gamma-ray source with HgI_2 Frisch collar device biased at 1500 V. The device was probed with the highly collimated source along the central line at points 1 through 6 for 4 h real counting time at each point.

device at 1500 V results in the estimated values of electron and hole mobility-lifetime products $\mu_{e,h}\tau_{e,h}$ of 0.0008 and 0.00003 $cm^2 \cdot V^{-1}$, respectively, for the HgI_2 crystal.[16] The $\mu_{e,h}\tau_{e,h}$ values for the HgI_2 were evaluated by a trial-and-error method to fit the best CCE profile through

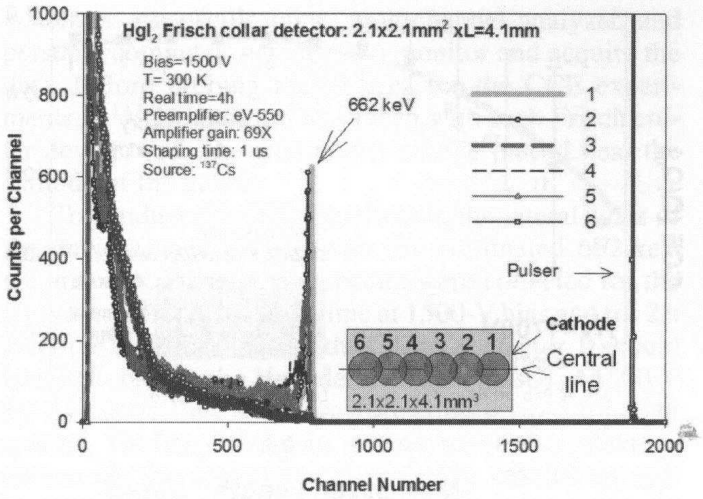

Fig. 10. Pulse-height spectra collected from the collimated ^{137}Cs gamma-ray source with the HgI_2 Frisch collar device.

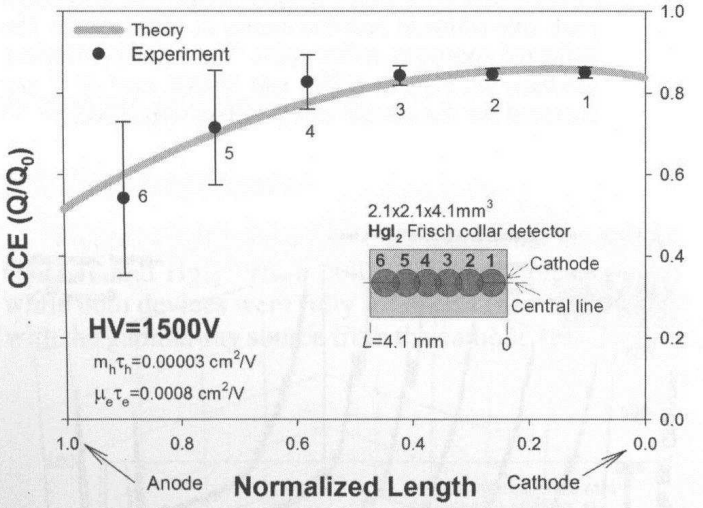

Fig. 11. The CCE profile along the central line of the HgI_2 Frisch collar device biased at 1500 V. The experimental data points are the normalized peak channel of the photopeak for the irradiated points (1 through 6) of the Frisch collar device. The error bars represent the photopeak full-width at half-maximum at 662 keV. For the best CCE profile, the mobility-lifetime products $\mu_{e,h}\tau_{e,h}$ of 0.0008 and 0.00003 $cm^2 \cdot V^{-1}$ are estimated for the electrons and holes, respectively.

the peak channel of the photopeak, as presented in Fig. 11. These $\mu_{e,h}\tau_{e,h}$ values for HgI_2 crystals are comparable to the commercially available HgI_2 crystals grown by Constellation Technology, as reported to be 0.0002 and 0.00005 $cm^2 \cdot V^{-1}$, for electrons and holes, respectively.[17] It should be noted that because of the significantly higher resistivity of HgI_2 materials to that of CdZnTe, the fabricated HgI_2 detector can withstand a higher electric field before reaching a breakdown voltage.

V. SUMMARY

The CCEs of a 7.8- × 7.8- × 15.6-mm^3 CdZnTe Frisch collar detector and a 2.1- × 2.1- × 4.1-mm^3 HgI_2 Frisch collar detector were measured by probing both devices with highly collimated 662-keV gamma rays. The experimental results showed uniform CCEs in more than half of the device volumes (consistent peak channel of photopeak). The experimental results were confirmed through the simulation of the CdZnTe Frisch collar device and the theoretical prediction of the CCE profiles (Fig. 8) with known values of the mobility-lifetime products for electrons and holes in CdZnTe ($\mu_e\tau_e$ = 0.045 $cm^2 \cdot V^{-1}$ and $\mu_h\tau_h$ = 0.0001 $cm^2 \cdot V^{-1}$). Similarly, for the HgI_2 detector the experimental results were confirmed with the simulation of the device and the prediction of the CCE profiles with $\mu_e\tau_e = 0.0008$ $cm^2 \cdot V^{-1}$ and $\mu_h\tau_h = 0.00003$ $cm^2 \cdot V^{-1}$. Despite equal aspect ratios for both devices in this study, and a shorter length for the HgI_2 Frisch collar detector, the CdZnTe Frisch collar device performs better than its HgI_2 counterpart. This advantage is mainly due to the better electron and hole mobility-lifetime products of CdZnTe. Nevertheless, the spectroscopic performance of both CdZnTe and HgI_2 devices in planar configurations showed significant improvement with the Frisch collars applied.

ACKNOWLEDGMENT

This work was supported by DTRA contracts HDTRA-1-07-1-007.

REFERENCES

1. D. McGREGOR, Z. HE, H. SEIFERT, D. WEHE, and R. ROJESKI, "Single Charge Carrier Type Sensing with a Parallel Strip Pseudo-Frisch-Grid CdZnTe Semiconductor Radiation Detector," *Appl. Phys. Lett.*, **72**, 7, 792 (1998).

2. E. ARIESANTI, A. KARGAR, and D. S. McGREGOR, "Fabrication and Spectroscopy Results of Mercuric Iodide Frisch Collar Detectors," *Nucl. Instrum. Methods A.*, **3**, 3, 656 (2010).

3. A. KARGAR, A. BROOKS, M. HARRISON, H. CHEN, S. AWADALLA, G. BINDLEY, B. REDDEN, and D. McGREGOR, "Uniformity of Charge Collection Efficiency in Frisch Collar Spectrometer with THM Grown CdZnTe Crystals," *SPIE Proc.*, **7449**, 744908 (2009).

4. A. KARGAR, A. BROOKS, M. HARRISON, H. CHEN, S. AWADALLA, G. BINDLEY, and D. McGREGOR, "Effect of Crystal Length on CdZnTe Frisch Collar Device Performance," *IEEE Nucl. Sci. Conf. R.*, 2017 (2009).

5. A. KARGAR, R. B. LOWELL, M. J. HARRISON, and D. S. McGREGOR, "The Crystal Geometry and the Aspect

Ratio Effects on Spectral Performance of CdZnTe Frisch Collar Device," in *SPIE Proc.*, **6706**, 67061J (2007).

6. J. E. BACIAK and Z. HE, "Comparison of 5 and 10 mm Thick HgI2 Pixelated γ-Ray Spectrometers," *Nucl. Instrum. Methods A.*, **505**, *1–2*, 191 (2003).

7. W. KAYE, J. BERRY, F. ZHANG, and Z. HE, "Depth Reconstruction Validation in Pixelated Semiconductor Detectors," *IEEE Nucl. Sci. Conf. R.*, 1768 (2009).

8. W. SHOCKLEY, "Currents to Conductors Induced by a Moving Point Charge," *J. Appl. Phys.*, **9**, 635 (1938).

9. S. RAMO, "Currents Induced by Electron Motion," *IRE Proc.*, **27**, 584 (1939).

10. M. J. HARRISON, A. KARGAR, and D. S. McGREGOR, "Charge Collection Characteristics of Frisch Collar CdZnTe Gamma-Ray Spectrometers," *Nucl. Instrum. Methods A*, **579**, *1*, 134 (2007).

11. A. KARGAR, "CdZnTe Frisch Collar Spectrometer Characterization, Optimization and Its Application in Array of Detectors," PhD Thesis, Kansas State University (2009).

12. A. KARGAR, M. J. HARRISON, A. C. BROOKS, and D. S. McGREGOR, "Characterization of Charge Carrier Collection in a CdZnTe Frisch Collar Detector with a Highly Collimated ^{137}Cs Source," *Nucl. Instrum. Methods Phys. Res. A.*, **620**, 270 (2010).

13. A. KARGAR, A. C. BROOKS, M. J. HARRISON, K. T. KOHMAN, R. B. LOWELL, R. C. KEYES, H. CHEN, G. BINDLEY, and D. S. McGREGOR, "The Effect of the Dielectric Layer Thickness on Spectral Performance of CdZnTe Frisch Collar Gamma Ray Spectrometers," *IEEE Trans. Nucl. Sci.*, **56**, *3*, 824 (2009).

14. Redlen Technologies: http://www.redlen.com/.

15. A. KARGAR, A. M. JONES, W. J. McNEIL, M. J. HARRISON, and D. S. McGREGOR, "CdZnTe Frisch Collar Detectors for γ-Ray Spectroscopy," *Nucl. Instrum. Methods A*, **558**, *2*, 497 (2006).

16. A. KARGAR, E. ARIESANTI, S. JAMES, and D. S. McGREGOR, "Charge Collection Efficiency Characterization of a HgI_2 Frisch Collar Spectrometer with Collimated High Energy Gamma Rays," *Nucl. Instrum. Methods A.*, doi:10.1016/j.nima.2010.08.057 (2010).

17. Constellation Technology: http://www.contech.com.